Efficient computation of forces on dislocation segments in anisotropic elasticity

Jie Yin[1]**, David M Barnett**[1,2] **and Wei Cai**[2]

[1] Department of Materials Science and Engineering, Stanford University, Stanford, CA 94305-4040, USA
[2] Department of Mechanical Engineering, Stanford University, Stanford, CA 94305-4040, USA

Abstract

We compare several alternative approaches for computing the stress field of a straight dislocation segment and its forces on other segments in an anisotropic linear elastic medium. The Willis–Steeds–Lothe expression can be implemented faster than Brown's formula and the matrix formalism is only slightly faster than the integral formalism. Expressions for self-stress and self-force are also explicitly derived. As an example, the critical stress to activate a Frank–Read source is computed as a function of its length in both isotropic and anisotropic materials.

(Some figures in this article are in colour only in the electronic version)

1. Introduction

Dislocation dynamics (DD) simulations have been developed to link the plastic deformation of single crystals with the microscopic dynamics of dislocations. Most of the existing DD simulation programs are limited to isotropic elasticity [1–3], even though most single crystals are elastically anisotropic. The elastic anisotropy may become very large under certain conditions, such as high temperature or high pressure. For example, as a nuclear reactor structural material, iron becomes highly anisotropic at high temperature [4]. Understanding the connection between DD and plasticity under these conditions requires an efficient DD simulation program that can account for anisotropic elasticity.

The anisotropic elasticity theory of dislocations was developed several decades ago (see for example, [5]). Similar to the case of isotropic elasticity, the stress field of a dislocation line can be written as a line integral. Unfortunately, in general the explicit expression for the integrand does not exist, because there is no closed-form solution of the elastic Green function in generally anisotropic media. Computing the integrand in the dislocation stress field expression in anisotropic elasticity requires the calculation of an extra integral (as in the integral formalism [7, 8]) or an auxiliary eigenvalue problem (as in the matrix formalism [5, 8]). Several attempts have been made to develop DD simulation programs applicable in anisotropic

elasticity [6, 7], but the computational speed is much lower than DD simulations using only isotropic elasticity. Because modeling crystal plasticity using DD simulations in isotropic elasticity already poses a great computational challenge, extending this type of simulation to anisotropic elasticity requires us to significantly improve the computational efficiency of existing implementations.

The main purpose of this paper is to compare several theoretical approaches for computing the stress field of dislocation segments and to identify the approach that is best suited for DD simulations in terms of numerical accuracy and efficiency. The paper is organized as follows. In section 2, we introduce the Brown and the Willis–Steeds–Lothe formulae for the stress field of straight dislocation segments and present our approach to compute forces on dislocation nodes. In section 3, we compare the accuracy and efficiency of several methods and present simulation results for the critical stress to activate a Frank–Read (FR) dislocation source in an isotropic and an anisotropic elastic medium.

2. Method

In DD simulations the dislocation line is usually discretized and is represented as a set of nodes connected by short straight segments [1, 2] or cubic splines [6]. For simplicity, in this paper we focus on the case of straight segments. At every time step, forces on the discretization nodes are computed, based on which the nodal velocities are computed using a mobility law. Because the forces on a dislocation are proportional to the local stress, the first step in deriving the interaction forces is to obtain the stress field generated by a dislocation segment. In the following, we first give a brief review of the existing theories on the stress field of a dislocation segment in an anisotropic elastic medium. We then describe how to obtain interaction forces on the end nodes of the dislocation segment, including the self-force.

2.1. Stress field of an infinite straight dislocation

Consider an infinitely long straight dislocation passing through the origin and parallel to a unit vector t (the dislocation tangent vector), with Burgers vector b. We are interested in its stress field at an arbitrary point x. Choose two unit vectors m and n such that m, n and t form a right-handed coordinate system and x is contained in the m–t plane [5, 8], as shown in figure 1. The stress field of this infinite dislocation line at point x can be written as [5]

$$\sigma_{mn}^{\infty}(x, t, b) = \frac{1}{d} \Sigma_{mn}(m, t, b), \tag{1}$$

where the superscript ∞ indicates this is an infinite dislocation line, Σ_{mn} is the angular stress factor and d is the shortest distance from the field point x to the dislocation line (see figure 1). The orientations of m and n depend on both x and t. The angular stress factor Σ_{mn} can be expressed as [5]

$$\Sigma_{mn}(m, t, b) = \frac{1}{2\pi} C_{mnip} b_s \{-m_p S_{is} + n_p (nn)_{ik}^{-1}[B_{ks} + (nm)_{kr} S_{rs}]\}, \tag{2}$$

where for any two real unit vectors a and r

$$(ar)_{jk} \equiv a_i C_{ijkl} r_l \tag{3}$$

and $(nn)^{-1}$ is the inverse of (nn). C_{ijkl} is the elastic stiffness tensor of the anisotropic medium. The matrices Q, B and S only depend on C_{ijkl} and the dislocation direction t. Q_{ij} is the angular part of the elastic Green's tensor and $B_{ij} b_i b_j$ is the energy prefactor of a straight dislocation line with Burgers vector b. Q, B and S can be evaluated [5] using both the matrix formalism
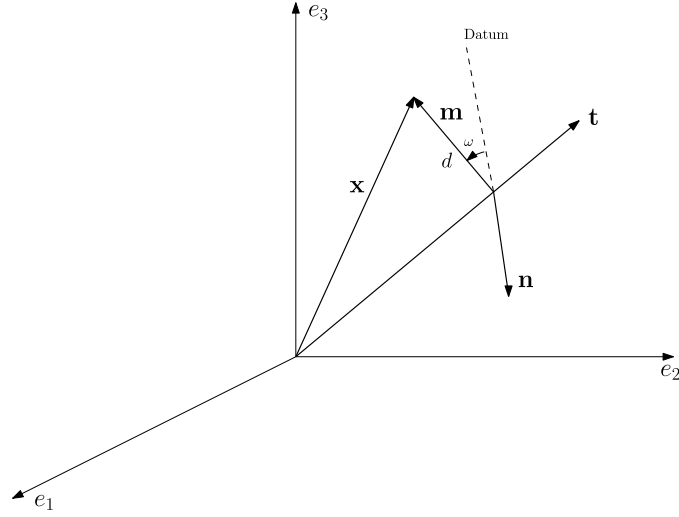
Figure 1. The relationship between m–n–t coordinate system and e_1–e_2–e_3 crystal coordinate system. The datum is an arbitrary line in the m–n plane [8].

(also called sextic formalism, which involves solving a six-dimensional eigen-equation [8, 10]) and the integral formalism [7, 8]. Both formalisms are summarized in appendix A.

Alternatively, we can compute the stress field from the displacement gradient (i.e. strain field),

$$\sigma_{ij}^{\infty}(\boldsymbol{x}, \boldsymbol{t}, \boldsymbol{b}) = C_{ijkl}\, u_{k,l}(\boldsymbol{x}, \boldsymbol{t}, \boldsymbol{b}), \tag{4}$$

where $u_{k,l} \equiv \partial u_k / \partial x_l$. The Willis–Steeds–Lothe formula [11] for the displacement gradient of an infinitely long dislocation segment is

$$u_{m,s}^{\infty} = \frac{1}{2\pi d}\epsilon_{jsn}b_i C_{ijkl}t_n\{-m_l Q_{mk} + n_l[(nn)^{-1} \cdot (nm) \cdot Q]_{mk} + n_l[(nn)^{-1} \cdot S^T]_{mk}\}, \tag{5}$$

where ϵ_{ijk} is a permutation tensor. Although they look different, equations (1) and (2) and equations (4) and (5) are equivalent and give identical numerical results.

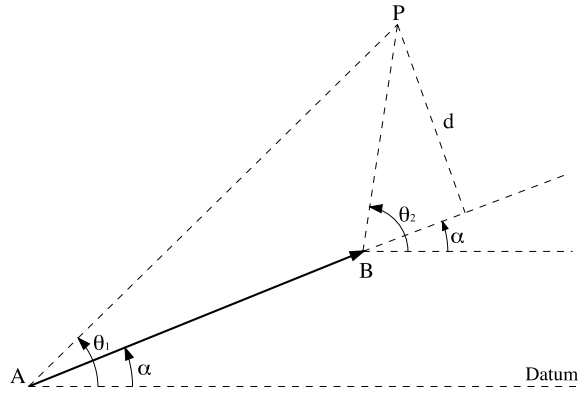## 2.2. Stress field of a finite dislocation segment

2.2.1. Brown's formula. To enable DD simulations in three dimensions, we need to be able to compute the stress field of an arbitrarily oriented finite dislocation segment. Fortunately, Brown's formula shows that the latter can be expressed in terms of quantities related to the stress fields of infinite dislocations given in the previous section [5].

The stress field of a finite, straight dislocation segment $\boldsymbol{AB}$ at point $\boldsymbol{P}$, as specified in figure 2, can be expressed as

$$\sigma_{ij} = \frac{1}{2d}[-\cos(\theta - \alpha)\Sigma_{ij}(\theta) + \sin(\theta - \alpha)\Sigma_{ij}'(\theta)]\Big|_{\theta_1}^{\theta_2}, \tag{6}$$

where Σ_{ij} is the angular stress factor of an infinite straight dislocation along $\boldsymbol{AP}$ or $\boldsymbol{BP}$. Σ_{ij}' is its derivative with respect to the angle θ and can be expressed in terms of angular derivatives of $\boldsymbol{B}$ and $\boldsymbol{S}$ [11].

$$\frac{\partial \Sigma_{mn}}{\partial \theta} = \frac{1}{2\pi}C_{mnip}b_s\left\{t_p S_{is} - \frac{\partial t_p}{\partial \theta}\frac{\partial S_{is}}{\partial \theta} + n_p(nn)_{ik}^{-1}\left[\frac{\partial B_{ks}}{\partial \theta} + \left(n\frac{\partial t}{\partial \theta}\right)_{kr}\frac{\partial S_{rs}}{\partial \theta} - (nt)_{kr}S_{rs}\right]\right\}.$$
$$\tag{7}$$

3

Figure 2. The geometry pertinent to Brown's formula. Consider a plane containing the straight segment AB and the field point P. α is the angle between the segment AB and an arbitrary (but fixed) datum in the same plane. θ_1 and θ_2 measure the orientations of line AP and line BP, relative to the datum, respectively.

Expressions for angular derivatives of matrices Q, B and S are given in appendix B. It is easy to show that as the length of the segment goes to infinity, $\theta_1 \to \alpha$ and $\theta_2 \to \alpha + \pi$, and equation (6) reduces to the stress field of an infinite dislocation line given by equation (1). Unlike the stress field of an infinite dislocation line, the stress field of a finite dislocation segment, such as that given in equation (6), is not unique, since any term which sums to zero around a closed polygonal loop may be added to equation (6).

The case of P collinear with segment AB but not on AB requires special attention because $d = 0$. It is easily shown that the stress field given by Brown's formula is zero in this case.

Brown's formula was used in an earlier implementation [7] of DD simulations in an anisotropic medium. Alternatively, one can also compute the stress field of a finite dislocation segment based on Mura's formula [9], but this requires numerical integration of the derivatives of Green's function over the dislocation segment [6]. This is less efficient than using Brown's formula or the Willis-Steeds–Lothe formula (see below), in which this integral has been performed analytically over straight segments. Therefore, we will not discuss the possible implementation based on Mura's formula any further.

2.2.2. Willis–Steeds–Lothe Formula. The stress field of a finite segment can also be obtained through the Willis–Steeds–Lothe formula for the displacement gradient [11],

$$\frac{\partial u_m}{\partial x_s} = \frac{1}{4\pi d}\epsilon_{jsn}b_i C_{ijkl}t_n \ \{-m_l Q_{mk} + n_l[(nn)^{-1}\cdot(nm)\cdot Q]_{mk} + n_l[(nn)^{-1}\cdot S^T]_{mk}\}\big|_{AP}^{BP} ,$$

(8)

where d is the shortest distance from field point x to the dislocation line pointing along t.

The original Willis–Steeds formula [12, 13] is not really useful for numerical work, while Lothe's reworking [11] of their result turns out to be extremely useful for numerical evaluation. As mentioned in the previous section, the Willis–Steeds–Lothe formula gives a different stress field from Brown's formula for a dislocation segment. The two formulae become equivalent only for complete dislocation loops. In comparison with Brown's formula, the Willis–Steeds–Lothe formula seems more convenient in that it avoids the calculation of Σ', which would require evaluation using a more cumbersome formula. As shown in section 3,
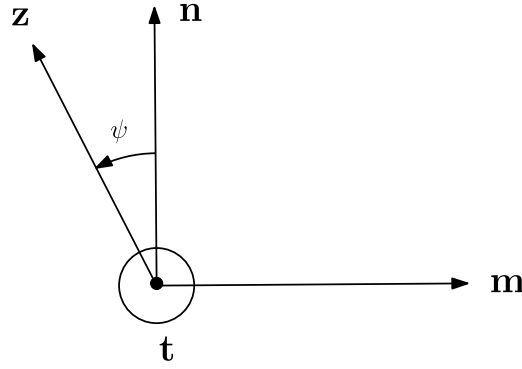
Figure 3. The geometric setup to derive the stress field using the Willis–Steeds–Lothe formula in the collinear case. z is an arbitrary unit vector in the m–n plane at an angle ψ from n.

the Willis–Steeds–Lothe formula leads to a faster calculation of the dislocation stress field than Brown's. It is easy to show that as the length of the segment goes to infinity, equation (8) reduces to equation (5).

Unlike the case of Brown's formula, the stress field using the Willis–Steeds–Lothe formula is non-zero in the collinear limit $d = 0$ (with the field point not on the segment). The displacement gradient in the collinear limit is [3]

$$\frac{\partial u_m}{\partial x_s}\bigg|_{d\to 0} = \left(\frac{1}{r_2} - \frac{1}{r_1}\right) \cdot \frac{1}{4\pi}\epsilon_{jsn}b_i C_{ijkl}t_n \left\{ t_l Q_{mk} - m_l \cdot \frac{\partial Q_{mk}}{\partial \theta} \right.$$

$$\left. + n_l \left[(nn)^{-1}(-nt) \cdot Q + (nn)^{-1}(nm) \cdot \frac{\partial Q}{\partial \theta} + (nn)^{-1} \cdot \frac{\partial S^T}{\partial \theta} \right]_{mk} \right\}, \tag{9}$$

where $r_1 = |AP|$, $r_2 = |BP|$. Hence, as $d \to 0$, the derivatives of the matrices Q and S are required. By symmetry, the result should only depend on t as long as m–n–t forms a right-handed coordinate system. This expression reduces to a form that is independent from m and n using the integral formalism (geometry shown in figure 3)

$$\frac{\partial u_i}{\partial x_p}\bigg|_{d\to 0} = \frac{1}{8\pi^2}\epsilon_{pjw}b_m C_{wmrs}t_j \left(\frac{1}{r_2} - \frac{1}{r_1}\right)$$

$$\times \int_0^{2\pi} (t_s(zz)_{ir}^{-1} - z_s[(zz)^{-1}((tz) + (zt))(zz)^{-1}]_{ir})\mathrm{d}\psi. \tag{10}$$
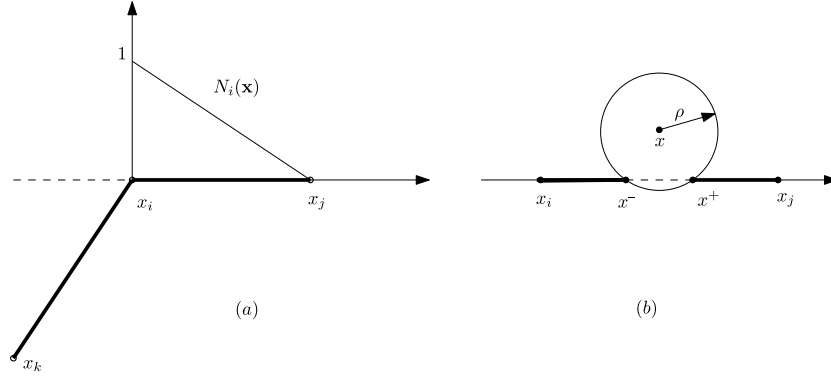
Hence the stress field at collinear point P is

$$\sigma_{kl}^{WS}(P) = \left(\frac{1}{|AP|} - \frac{1}{|BP|}\right) g_{kl}(t), \tag{11}$$

where

$$g_{kl}(t) = \frac{1}{8\pi^2}C_{klip}\epsilon_{pjw}b_m C_{wmrs}t_j \tag{12}$$

$$\int_0^{2\pi} (t_s(zz)_{ir}^{-1} - z_s[(zz)^{-1}((tz) + (zt))(zz)^{-1}]_{ir})\,\mathrm{d}\psi. \tag{13}$$

---

[3] The derivation of equations (9) and (10) is yet to be published. The authors are willing to provide details to interested readers by email.

Figure 4. (*a*) Two connected segments, *i*–*k* and *i*–*j*. $N_i(\boldsymbol{x})$ is the shape function; (*b*) illustration of cut-off convention for a field point $\boldsymbol{x}$ close to segment $\boldsymbol{x}_i$–$\boldsymbol{x}_j$. The portion of this segment outside the cut-off radius ρ consists of two segments $\boldsymbol{x}_i$–$\boldsymbol{x}^-$ and $\boldsymbol{x}^+$–$\boldsymbol{x}_j$.

2.3. Nodal forces

For a dislocation line that is discretized into straight segments connecting a set of nodes, the force on a node is the weighted integral of the Peach–Koehler force on its neighboring segments. For example, the force on node *i* due to segment *i*–*j* is [14], see figure 4(*a*),

$$F_i^{(ij)} = \int_{\boldsymbol{x}_i}^{\boldsymbol{x}_j} N_i(\boldsymbol{x})\, \boldsymbol{f}^{\text{PK}}(\boldsymbol{x})\, \mathrm{d}l(\boldsymbol{x}), \tag{14}$$

where shape function $N_i(\boldsymbol{x})$ goes linearly from 1 at $\boldsymbol{x}_i$ to 0 at its neighbors, i.e.

$$N_i(\boldsymbol{x}) = \frac{|\boldsymbol{x} - \boldsymbol{x}_j|}{|\boldsymbol{x}_j - \boldsymbol{x}_i|}. \tag{15}$$

$\boldsymbol{f}^{\text{PK}}$ is the Peach–Koehler force,

$$\boldsymbol{f}^{\text{PK}}(\boldsymbol{x}) \equiv (\boldsymbol{\sigma}(\boldsymbol{x}) \cdot \boldsymbol{b}) \times \boldsymbol{\xi}, \tag{16}$$

where $\boldsymbol{\sigma}$ is the local stress at field point $\boldsymbol{x}$ on segment *i*–*j*, $\boldsymbol{b}$ is the Burgers vector of segment *i*–*j* and $\boldsymbol{\xi}$ is its line direction. The stress field $\boldsymbol{\sigma}$ is the superposition of the contributions from externally applied stress, dislocation segments other than *i*–*j* and the segment *i*–*j* itself (self-stress), i.e.

$$\boldsymbol{\sigma}(\boldsymbol{x}) = \boldsymbol{\sigma}^{\text{ext}} + \sum_{k,l \neq i,j} \boldsymbol{\sigma}^{(kl)}(\boldsymbol{x}) + \boldsymbol{\sigma}^{(ij)}(\boldsymbol{x}). \tag{17}$$

Because each stress field has a different spatial variation, its contribution to the integral in equation (14) will be evaluated separately, i.e.

$$F_i^{(ij)} = F_i^{(ij),\text{ext}} + \sum_{k,l \neq i,j} F_i^{(ij),(kl)} + F_i^{(ij),\text{self}}. \tag{18}$$

When the externally applied stress is a constant, its contribution is

$$F_i^{(ij),\text{ext}} = \tfrac{1}{2}\, (\boldsymbol{\sigma}^{\text{ext}} \cdot \boldsymbol{b}) \times (\boldsymbol{x}_j - \boldsymbol{x}_i). \tag{19}$$

The contribution from the stress field of another segment *k*–*l* can be expressed as

$$F_i^{(ij),(kl)} = \int_{\boldsymbol{x}_i}^{\boldsymbol{x}_j} N_i(\boldsymbol{x})\, (\boldsymbol{\sigma}^{kl}(\boldsymbol{x}) \cdot \boldsymbol{b}) \times \boldsymbol{\xi}\, \mathrm{d}l(\boldsymbol{x}). \tag{20}$$

This integral has to be evaluated numerically and the number of integration points is chosen automatically to reach a specified tolerance. We used the adaptive Simpson's method (function quadv in Matlab) to calculate the integral.

To avoid a singularity, we apply a cut-off when field point x is within a distance ρ from any dislocation segment. As shown in figure 4(*b*), the stress field due to segment $x_i - x_j$ is the summation of the stress field of segment $x_i - x^-$ and that of $x^+ - x_j$. The contribution from segment $x^- - x^+$ is removed because it is entirely within the cut-off radius ρ around point x.

When we evaluate the nodal force contribution due to the stress field of segment $i - j$ itself, we first need to obtain the stress of segment $i - j$ on itself. In the collinear limit, by applying the results of the Willis–Steeds–Lothe formula and our cut-off convention, we obtain the following self-stress expression (assuming $L \equiv |x_j - x_i| > 2\rho$),

$$\sigma^{(ij)}(x) = \begin{cases} \left(\dfrac{1}{|x - x_i|} - \dfrac{1}{|x - x_j|} \right) g(\xi) & |x - x_i| > \rho \ \text{and} \ |x - x_j| > \rho, \\[3mm] \left(\dfrac{1}{\rho} - \dfrac{1}{|x - x_j|} \right) g(\xi) & |x - x_i| < \rho, \\[3mm] \left(\dfrac{1}{|x - x_i|} - \dfrac{1}{\rho} \right) g(\xi) & |x - x_j| < \rho, \end{cases} \tag{21}$$

where g is the tensor defined in equation (11). Thus the self-force contribution to node i is

$$\begin{aligned} F_i^{(ij),\text{self}} &= \int_{x_i}^{x_j} N_i(x) \left(\sigma^{ij}(x) \cdot b \right) \times \xi \, \mathrm{d}l(x) \\ &= G(\xi) \, P(L, \rho), \end{aligned} \tag{22}$$

where

$$G(\xi) = (g(\xi) \cdot b) \times \xi. \tag{23}$$

$G(\xi)$ is the orientation dependent part of the self-force, and

$$\begin{aligned} P(L, \rho) &= \int_0^L \frac{L - x}{L} \left[\min\left(\frac{1}{x}, \frac{1}{\rho} \right) - \min\left(\frac{1}{L - x}, \frac{1}{\rho} \right) \right] \mathrm{d}x \\ &= \ln \frac{L}{\rho} + \frac{\rho}{L} - 1 \end{aligned} \tag{24}$$

is the length dependent part of the self-force (assuming $L > 2\rho$). Therefore we have greatly simplified the computation of self-force using the Willis–Steeds–Lothe formula.

3. Results

In this section, we first compare the efficiencies and accuracies of various alternatives of stress field calculation methods and then performed DD simulations of a FR Source. The calculations are performed by Matlab codes [15] running on a 2.8 GHz desktop PC.

3.1. Stress field of infinite dislocation line

As mentioned in section 3, we can compute the Q, B and S matrices using either the matrix or the integral formalism. Since Brown's formula is equivalent to the Willis–Steeds–Lothe formula for an infinite dislocation line, here we only investigate Brown's formula. To evaluate the accuracy of various methods, in isotropic medium, we compare our numerical results with the result given by analytic expression based on isotropic elasticity [10]. For an anisotropic medium, however, we set as a reference the stress field given by integral formalism with 10^4

Table 1. Computational efficiency and accuracy of different formalisms for computing the stress field of an infinite dislocation. N_{int} is the number of integration points used in the integral formalism. In isotropic medium tungsten (W), $C_{11} = 521$ GPa, $C_{12} = 201$ GPa, $C_{44} = 160$ GPa, $\mu = C_{44}$, $\nu = C_{12}/(C_{11} + C_{12})$. In the anisotropic medium molybdenum (Mo), $C_{11} = 460$ GPa, $C_{12} = 176$ GPa, $C_{44} = 110$ GPa.

W (iso)	Matrix	$N_{int} = 5$	$N_{int} = 11$	$N_{int} = 21$
Time (s)	4.2e−4	4.5e−4	6.6e−4	1.0e−3
Relative error	3.2e−8	6.6e−16	1.1e−16	2.2e−16
Mo (aniso)	Matrix	$N_{int} = 5$	$N_{int} = 11$	$N_{int} = 21$
Time (s)	4.1e−4	4.5e−4	6.6e−4	1.0e−3
Relative error	5.8e−15	6.2e−4	3.5e−8	2.9e−15

integration points. All calculations are performed for the stress field at point $x = [3\,5\,\overline{7}]$ due to an infinite dislocation line passing through the origin along the [1 3 4] direction with Burgers vector $b = \frac{1}{2}[1\,\overline{2}\,1]$.

Table 1 compares the accuracy and efficiency of various approaches to compute the stress field at point x. We note that in tungsten, which is elastically isotropic, the eigenvalue problem involved in the matrix formalism becomes non-semi-simple degenerate and one cannot numerically obtain meaningful answers unless the elastic constants are slightly perturbed away from isotropy. In our test case, we perturb C_{44} (on the order of 100 GPa) by 1 MPa and the perturbation does not have an appreciable influence on the final stress results, as indicated by the negligible error (3.2e−8) when compared with analytic solutions in isotropic elasticity. We can see from table 1 that, in both media, the application of matrix formalism is slightly faster than the integral formalism. We also note that the integral formalism converges rapidly with respect to N_{int}. Only five integration points suffice to reach an accuracy of 0.1%.

In summary, the matrix formalism is only slightly faster than the integral formalism for computations involving infinite straight dislocations. The integral formalism is competitive and is also easier to implement. It is worthwhile to note that the relative computational efficiency may be biased by the use of the Matlab program, whose internal eigenvalue solver is highly efficient. When the algorithms are implemented in a C program, we shall need to compare the computational efficiencies again[4].

3.2. Stress field of polygonal dislocation loop

Since the stress field of a finite segment is not unique, in order to compare Brown's and Willis–Steeds–Lothe formulae, we consider the stress field of a complete polygonal dislocation loop $ABDE$ at point P in both isotropic (W) and anisotropic (Mo) media, where $A = [1\,3\,3]$, $B = [3\,1\,5]$, $D = [5\,3\,2]$, $E = [3\,7\,4]$ and $P = [3\,2\,6]$. The Burgers vector is $b = [1\,2\,\overline{1}]$. Tables 2 and 3 compare the time and accuracy of various methods. We used the same references as the previous test case to compute relative errors in both isotropic and anisotropic media.

One observes that matrix formalism is still slightly faster than integral formalism. However, when the same formalism is applied in both isotropic and anisotropic media to compute Q, B and S, the Willis–Steeds–Lothe formula leads to much higher efficiency than Brown's formula (by about a factor of 3) without losing accuracy. The acceleration is due to the absence of angular derivative terms in the Willis–Steeds–Lothe formula. Hence, the

---

[4] Anisotropic elasticity algorithms based on the Willis–Steeds–Lothe formula and the integral formalism have been implemented in C for the ParaDiS program [1] by Drs Sylvie Aubry and Steven P Fitzgerald.

Table 2. Computational time and accuracy of various methods to compute the stress field of a dislocation loop $ABDE$ at point P in W (isotropic). WSL is short for the Willis–Steeds–Lothe formula and N_{int} is the number of integration points in integral formalism.

Brown	Matrix	$N_{int} = 5$	$N_{int} = 11$	$N_{int} = 21$
Time (s)	1.2e−2	2.3e−2	2.9e−2	4.2e−2
Relative error	9.3e−7	4.9e−16	4.4e−16	1.8e−16
WSL	Matrix	$N_{int} = 5$	$N_{int} = 11$	$N_{int} = 21$
Time (s)	4.4e−3	4.7e−3	6.4e−3	9.1e−3
Relative error	7.7e−8	7.1e−16	2.2e−16	3.1e−16

Table 3. Computational time and accuracy of various methods to compute the stress field of a dislocation loop $ABDE$ at point P in Mo (anisotropic).

Brown	Matrix	$N_{int} = 5$	$N_{int} = 11$	$N_{int} = 21$
Time (s)	1.1e−2	3.3e−2	3.6e−2	4.2e−2
Relative error	6.7e−15	5.1e−4	3.4e−8	8.5e−15
WSL	Matrix	$N_{int} = 5$	$N_{int} = 11$	$N_{int} = 21$
Time (s)	4.2e−3	4.7e−3	6.3e−3	9.1e−3
Relative error	7.1e−15	1.6e−3	1.5e−8	2.7e−15

combination of the matrix formalism and the Willis–Steeds–Lothe is an efficient method to compute the stress field due to a dislocation segment.

3.3. FR source in infinite isotropic media

DDLab is a Matlab program for DD simulation in isotropic elasticity developed for pedagogical purposes [16]. We modified the Matlab subroutines for calculating segmental interactions and self-forces to make a DD program in anisotropic media [15]. To test the robustness of our anisotropic DD implementations, we simulated the FR source activation process and compared the critical stress for both screw and edge dislocations with isotropic DD results.

Figure 5 shows the initial configuration setup. A complete rectangular loop of height h is studied ($h = 4L$). By applying an external stress field (in steps of 1 MPa), the dislocation segment AB of length L bows out gradually and becomes a FR source. To detect whether the FR source is activated, we use a criterion that R must be larger than $2L$, where R is the maximum bowed out distance in the y-direction as shown in figure 5. To represent the bowing-out process, the segment AB is discretized into multiple shorter segments, for instance, $N_s = 10$.

We first studied a FR source in an isotropic medium (tungsten), where we can compare the results from a slightly anisotropic DD code with those from an isotropic DD code. In this test case, the Burgers vector magnitude is arbitrarily set to $|\boldsymbol{b}| = \frac{\sqrt{3}}{2}a_0$, where $a_0 = 0.3165$ nm. The cut-off radius in the anisotropic DD code is $\rho = 1$ nm. The core radius of the isotropic DD code [17] is also set to $a = 1$ nm.

Figure 6 depicts our numerical results of FR source critical stress. An initially screw dislocation segment exhibits a higher activation stress than does an initially edge dislocation segment. When the dislocation length L increases from 100 to 500 nm, its FR source activation stress decreases, a behavior captured by both isotropic DD and anisotropic DD codes. The plot shows that the results given by anisotropic DD codes are close to those given by isotropic
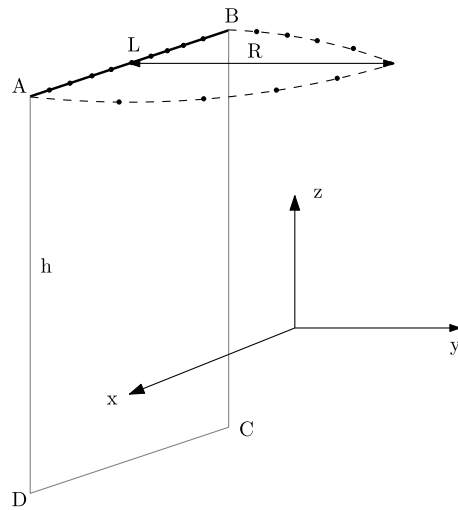
Figure 5. Initial configuration setup used to study FR source in an isotropic medium.
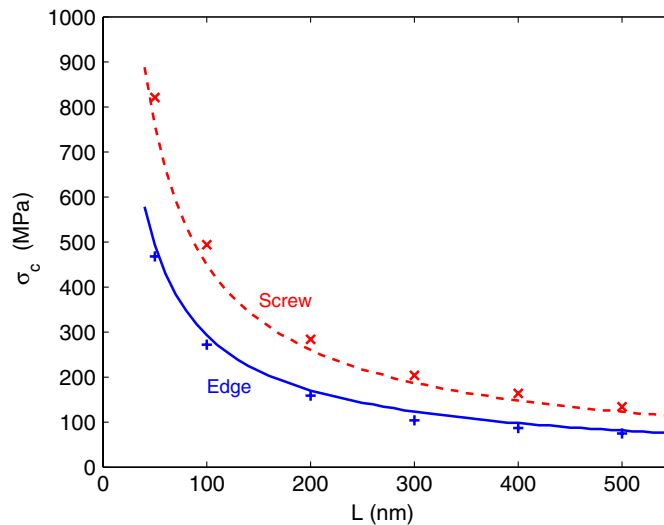

Figure 6. FR source activation stress for dislocation segments with different lengths in tungsten. Critical stresses predicted by isotropic DD code are plotted as solid and dashed lines for initially edge and screw dislocations, respectively. Critical stresses predicted by anisotropic DD code are plotted as + and × for initially edge and screw dislocations, respectively.

codes. This is interesting because the two programs use different cut-off schemes to avoid singularities. The isotropic DD program uses a non-singular dislocation theory where the dislocation line is spread out isotropically in space [17], while the anisotropic DD program uses the spherical truncation described in section 2.3.

We note that the ratio of the critical stress for the initially screw and initially edge dislocations predicted by both isotropic and anisotropic codes is $\sigma_c^{\text{screw}}/\sigma_c^{\text{edge}} \approx 1.5$. This is larger than the prediction from a line tension model[5], $\sigma_c^{\text{screw}}/\sigma_c^{\text{edge}} = 1/(1-\nu)$. For

---

[5] The line tension model [18] predicts that $\sigma_c^{\text{screw}}/\sigma_c^{\text{edge}} = E_e/E_s = 1/(1-\nu)$, where E_e and E_s are the energy prefactors of straight edge and screw dislocations, respectively.

Table 4. Effective isotropic elastic constants (μ, ν) based on different averaging schemes for anisotropic iron and the corresponding critical stress for a FR source with initially screw (σ_c^{screw}) and edge orientation (σ_c^{edge}).

Iron	μ (GPa)	ν	E_e/E_s	σ_c^{screw} (MPa)	σ_c^{edge} (MPa)	$\sigma_c^{screw}/\sigma_c^{edge}$
Reuss	73	0.419	1.72	227	121	1.88
Voigt	86	0.291	1.41	222	143	1.55
Scattergood	62.5	0.473	1.90	214	101	2.12
Aniso	—	—	1.90	222	92	2.41

tungsten $\nu = 0.278$, hence the line tension model would predict $\sigma_c^{screw}/\sigma_c^{edge} = 1.39$. We believe the line tension approximation is responsible for the differences observed here.

When segment **AB** is 100 nm and discretized into 10 segments, the anisotropic DD simulation requires a longer time than isotropic DD simulation by a factor of 220. This benchmark result is more favorable than the previous implementation where the anisotropic DD code is about 500 times slower than the isotropic DD code [7]. Furthermore, our ratio of 220 is obtained when comparing the anisotropic DD code with a highly efficient isotropic DD code, in which interaction forces between any two dislocation segments are computed based on analytic expressions without any numerical integration [1]. Hence our new implementation of the anisotropic DD simulation is faster than the earlier attempt [7] by more than a factor of 2. As mentioned above, the time measurements may be largely influenced by the peculiarities of Matlab and need to be repeated when the algorithm is implemented in C language.

3.4. FR source in infinite anisotropic media

We used a similar configuration as figure 5 to study FR Source activation in anisotropic media. For iron, with anisotropic elastic constants, $C_{11} = 242$ GPa, $C_{12} = 146.5$ GPa, $C_{44} = 112$ GPa, we computed the critical FR source activation stress for a 100 nm dislocation segment. The simulation is based on the following slip system, Burgers vector $\boldsymbol{b} = \frac{1}{2}[\bar{1}11]a_0$ and slip plane $\boldsymbol{n} = (110)$, where $a_0 = 0.2867$ nm. The cut-off radius is set to $\rho = 1$ nm. The results are given in table 4 under the heading 'Aniso'. The ratio between the activation stress of initially screw and initially edge dislocations is found to be $\sigma_c^{screw}/\sigma_c^{edge} = 2.41$. The energy prefactor for straight edge and screw dislocations on this slip system is $E_e/E_s = 1.90$. This would mean that a line tension model would predict $\sigma_c^{screw}/\sigma_c^{edge} = 1.90$, consistent with [19]. Hence the discrepancy between the predictions from a line tension model and full elasticity calculations is larger in the anisotropic DD code than that in the isotropic DD code.

Similar to the comparison performed in [6], we computed the critical FR source activation stress using the isotropic DD code. Three sets of average elastic constants are used, based on the average scheme of Reuss [10], Voigt [10] and Scattergood [20, 21]. The core radius is also set to $a = 1$ nm. The results are shown in table 4. One observes that the Scattergood scheme gives the best agreement with the anisotropic DD predictions. This is not surprising because by design the Scattergood scheme fits the effective isotropic elastic constants to the energy prefactor of purely edge (E_e) and pure screw dislocations (E_s) on a given slip system in the anisotropic medium [20, 21].

Figure 7 shows the critical configuration of the FR source predicted by anisotropic and isotropic DD codes. Again, the isotropic DD simulations using the effective elastic constants given by the Scattergood scheme give the closest agreement with anisotropic DD
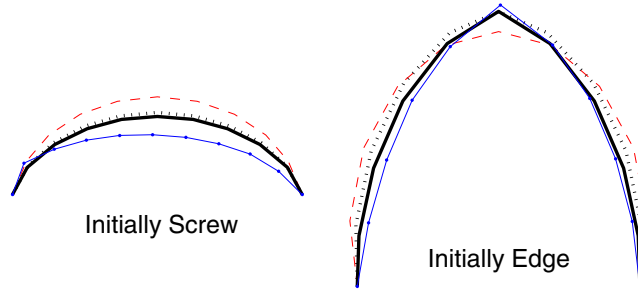
Figure 7. Critical configuration of a FR source in iron made of an initially screw and an initially edge dislocation segment that is 100 nm long. Anisotropic DD results (thin solid line) are compared with isotropic DD results with different effective elastic constants: Reuss (dotted line), Voigt (dashed line) and Scattergood (thick solid line).

simulations, consistent with an earlier report [6]. Moreover, the critical configuration predicted by anisotropic DD simulation no longer has the mirror symmetry possessed by isotropic DD predictions, illustrating the effect of elastic anisotropy.

4. Summary

We have implemented several methods to compute stresses and forces on dislocations in anisotropic media. The matrix formalism together with the Willis–Steeds–Lothe formula is found to be the most efficient. We also derived an analytical expression for the self-stress and self-force consistent with the spherical truncation scheme that we introduced. The new approach leads to much greater computational efficiency than before.

Acknowledgments

Appendix A. Expressions of Q, B and S in the matrix and integral formalisms

Consider an infinitely long dislocation line passing through the origin along unit vector t. Choose a local coordinate system m–n–t as in section 1. To obtain the stress field of this dislocation requires the solution of the following eigenvalue problem [8],

$$N \xi^\alpha = p_\alpha \xi^\alpha, \tag{A.1}$$

where N is a 6×6 matrix

$$N = - \begin{bmatrix} (nn)^{-1}(nm) & (nn)^{-1} \\ (mn)(nn)^{-1}(nm) - (mm) & (mn)(nn)^{-1} \end{bmatrix} \tag{A.2}$$

$(mn)_{jk} \equiv m_i C_{ijkl} n_l$ and $(mn)^{-1}$ is its inverse. $p_\alpha, \alpha = 1, \ldots, 6$ are the eigenvalues of matrix N, and form complex conjugate pairs. By convention, they are arranged in such a way that

p_4, p_5, p_6 are complex conjugates of p_1, p_2, p_3, and that $\text{Im}[p_\alpha] > 0$ for α=1,2,3. $\boldsymbol{\xi}^\alpha$ are the (6×1) eigenvectors that can be split into two 3×1 column vectors as

$$\boldsymbol{\xi}^\alpha = \begin{bmatrix} \boldsymbol{A}^\alpha \\ \boldsymbol{L}^\alpha \end{bmatrix}. \tag{A.3}$$

$\boldsymbol{A}^\alpha$ and $\boldsymbol{L}^\alpha$ are selected to satisfy the following orthonormal relations, namely,

$$\sum_{i=1}^3 A_i^\alpha L_i^\beta + A_i^\beta L_i^\alpha = \delta_{\alpha\beta}. \tag{A.4}$$

The $\boldsymbol{Q}$, $\boldsymbol{B}$ and $\boldsymbol{S}$ matrices can be expressed in terms of the normalized eigenvectors as

$$Q_{js} = i \sum_{\alpha=1}^6 \pm A_{j\alpha} A_{s\alpha} = 2i \sum_{\alpha=1}^3 A_{j\alpha} A_{s\alpha}, \tag{A.5}$$

$$B_{ij} = i \sum_{\alpha=1}^6 \pm L_{i\alpha} L_{j\alpha} = 2i \sum_{\alpha=1}^3 L_{i\alpha} L_{j\alpha}, \tag{A.6}$$

$$S_{ij} = i \sum_{\alpha=1}^6 \pm A_{i\alpha} L_{j\alpha} = i \left(\sum_{\alpha=1}^3 A_{i\alpha} L_{j\alpha} - \delta_{ij} \right). \tag{A.7}$$

They can also be expressed in the integral formalism as [7, 8]

$$Q_{js} = -\frac{1}{2\pi} \int_0^{2\pi} (nn)_{js}^{-1} \, d\omega, \tag{A.8}$$

$$B_{ij} = \frac{1}{2\pi} \int_0^{2\pi} \{(mm)_{ij} - (mn)_{ik}(nn)_{kp}^{-1}(nm)_{pj}\} \, d\omega, \tag{A.9}$$

$$S_{ij} = -\frac{1}{2\pi} \int_0^{2\pi} (nn)_{ik}^{-1}(nm)_{kj} \, d\omega, \tag{A.10}$$

where ω measures the rotation angle of the local coordinate system $\boldsymbol{m}$–$\boldsymbol{n}$–$\boldsymbol{t}$ around unit vector $\boldsymbol{t}$ (See figure 1). Even though the matrix $\boldsymbol{N}$ and its eigenvectors $\boldsymbol{A}$ and $\boldsymbol{L}$ depend on the choices of $\boldsymbol{m}$ and $\boldsymbol{n}$, the matrices $\boldsymbol{Q}$, $\boldsymbol{B}$, $\boldsymbol{S}$ only depend on vector $\boldsymbol{t}$, i.e. they are independent of $\boldsymbol{m}$ and $\boldsymbol{n}$. This can be seen from their expressions in the integral formalism. Because all integrands have a period of π, the matrices can be rewritten as integrals from 0 to π, decreasing the domain of numerical integration.

Appendix B. Angular derivatives of Q, B and S

In the matrix formalism, the angular derivatives of $\boldsymbol{Q}$, $\boldsymbol{B}$ and $\boldsymbol{S}$ can be obtained by studying the angular derivative of matrix $\boldsymbol{N}$ [8]. First, noticing that

$$\frac{\partial \boldsymbol{t}}{\partial \theta} = \boldsymbol{m}, \qquad \frac{\partial^2 \boldsymbol{t}}{\partial \theta^2} = -\boldsymbol{t} \tag{B.1}$$

we have

$$\frac{\partial \boldsymbol{N}}{\partial \theta} = \begin{bmatrix} (nn)^{-1}(nt) & 0 \\ q & (tn)(nn)^{-1} \end{bmatrix}, \tag{B.2}$$

where

$$q = (tn)(nn)^{-1}(nm) + (mn)(nn)^{-1}(nt) - (tm) - (mt). \tag{B.3}$$

13

The derivatives of the Stroh eigenvectors can then be obtained.

$$\frac{\partial \boldsymbol{\xi}^\beta}{\partial \theta} = \sum_{\substack{\alpha=1 \\ \alpha \neq \beta}}^{6} \frac{N_{\alpha\beta}^1}{p_\beta - p_\alpha} \boldsymbol{\xi}^\alpha, \tag{B.4}$$

where

$$N_{\alpha\beta}^1 = (\boldsymbol{\xi}^\alpha)^T \, \boldsymbol{T} \, \frac{\partial \boldsymbol{N}}{\partial \theta} \, \boldsymbol{\xi}^\beta, \tag{B.5}$$

$$\boldsymbol{T} = \begin{bmatrix} 0 & \boldsymbol{I} \\ \boldsymbol{I} & 0 \end{bmatrix}. \tag{B.6}$$

Recall that $\boldsymbol{\xi}^\alpha = \begin{bmatrix} \boldsymbol{A}^\alpha \\ \boldsymbol{L}^\alpha \end{bmatrix}$, this gives us the angular derivatives of both $\boldsymbol{A}$ and $\boldsymbol{L}$. The angular derivatives of $\boldsymbol{Q}$, $\boldsymbol{B}$ and $\boldsymbol{S}$ can now be expressed as follows:

$$\left(\frac{\partial \boldsymbol{Q}}{\partial \theta}\right)_{ij} = 2i \sum_{\alpha=1}^{3} \left(\frac{\partial A_i^\alpha}{\partial \theta} A_j^\alpha + A_i^\alpha \frac{\partial A_j^\alpha}{\partial \theta} \right), \tag{B.7}$$

$$\left(\frac{\partial \boldsymbol{B}}{\partial \theta}\right)_{ij} = 2i \sum_{\alpha=1}^{3} \left(\frac{\partial L_i^\alpha}{\partial \theta} L_j^\alpha + L_i^\alpha \frac{\partial L_j^\alpha}{\partial \theta} \right), \tag{B.8}$$

$$\left(\frac{\partial \boldsymbol{S}}{\partial \theta}\right)_{ij} = 2i \sum_{\alpha=1}^{3} \left(\frac{\partial A_i^\alpha}{\partial \theta} L_j^\alpha + A_i^\alpha \frac{\partial L_j^\alpha}{\partial \theta} \right). \tag{B.9}$$

References

[1] Arsenlis A, Cai W, Tang M, Rhee M, Oppelstrup T, Hommes G, Pierce T G and Bulatov V V 2007 *Modelling Simul. Mater. Sci. Eng.* **15** 553–95
[2] Schwarz K W 1999 *J. Appl. Phys.* **85** 108
[3] Zbib H M, Rhee M and Hirth J P 1998 *Int. J. Mech. Sci.* **40** 113–27
[4] Fitzgerald S P and Dudarev S L 2008 *Proc. R. Soc.* A **464** 2549–59
[5] Bacon D J, Barnett D M and Scattergood R O 1979 *Prog. Mater. Sci.* **23** 51–262
[6] Han X, Ghoniem N M and Wang Z 2003 *Phil. Mag.* **83** 3705–21
[7] Rhee M, Stolken J S, Bulatov V V, de la Rubia T D, Zbib H M and Hirth J P 2001 *Mater. Sci. Eng.* A **309–310** 288–93
[8] Lavagnino A M 1995 Selected Static and Dynamic Problems in Anisotropic Linear Elasticity *PhD Thesis* Stanford University
[9] Mura T 1991 *Micromechanics of Defects in Solids* 2nd edn (Dordrecht: Kluwer) p 47
[10] Hirth J P and Lothe J 1982 *Theory of Dislocations* 2nd edn (New York: Wiley)
[11] Lothe J 1992 Dislocations in anisotropic media *Elastic Strain Fields and Dislocation Mobility* ed V L Indenbom and J Lothe (*Series of Modern Problems in Condensed Matter Physics* vol 31) (Amsterdam: North-Holland)
[12] Willis J R 1970 *Phil. Mag.* **21** 931
[13] Steeds J W and Willis J R 1979 *Disocations in Anisotropic Media* ed F R N Nabarro (*Dislocations in Solids*) (Amsterdam: North-Holland) vol 1
[14] Bulatov V V and Cai W 2006 *Computer Simulations of Dislocations* (Oxford: Oxford University Press) chapter 10
[15] The Matlab programs implementing the algorithms in this paper can be downloaded at http://micro.stanford.edu/~caiwei/Forum
[16] The DDLab program can be downloaded at http://micro.stanford.edu/
[17] Cai W, Arsenlis A, Weinberger C R and Bulatov V V 2006 *J. Mech. Phys. Solids* **54** 561
[18] DeWit G and Koehler J S 1959 *Phys. Rev.* **116** 1113
[19] Fitzgerald S P 2010 *Phil. Mag. Lett.* **90** 209
[20] Scattergood R O and Bacon D J 1975 *Phil. Mag.* **31** 179
[21] Scattergood R O and Bacon D J 1982 *Acta Metall.* **30** 1665